Reactivity of a nitrosyl ligand on dinuclear ruthenium hydrotris(pyrazolyl)borato complexes toward a NO molecule

Yasuhiro Arikawa,* Ayumi Ikeda, Naoki Matsumoto and Keisuke Umakoshi

Received (in XXX, XXX) Xth XXXXXXXXX 20XX, Accepted Xth XXXXXXXXX 20XX
DOI: 10.1039/b000000x

A cationic mononitrosyl dinuclear ruthenium complex was prepared by removing one NO ligand of a dicationic dinitrosyl ruthenium complex using NaN_3. Reduction and oxidation reactions of the mononitrosyl complex led to the isolation of a neutral nitrosyl-bridged complex and a dicationic mononitrosyl complex, respectively, as expected from the cyclic voltammogram. According to the electron count, their reactions with a second NO molecule resulted in an N–N coupling complex from the nitrosyl-bridged complex and the dicationic dinitrosyl complex from the dicationic mononitrosyl complex.

Introduction

The NO ligand on transition metal complexes has attracted a great deal of attention because of its "non-innocent" property ($M–NO^+$, linear form; $M–NO^{\bullet}$ and $M–NO^-$, bent form). The transformations have been characterized by electrochemistry and IR, UV/Vis, and EPR spectroscopies,[1] but most of the reported complexes are mononitrosyl mononuclear systems. We have found two neighboring NO ligands on a dinuclear ruthenium complex $[\{TpRu(NO)\}_2(\mu\text{-Cl})(\mu\text{-pz})](BF_4)_2$ (**1**: $\{Ru_2(NO)_2\}^{12}$)[2] (Tp = HB(pyrazol-1-yl)$_3$) and its unprecedented redox behaviour (eqn (1)).[3] Reduction of the dicationic dinitrosyl ruthenium **1** induced an N-N bond formation of the two NO ligands, affording an N–N coupling complex $[(TpRu)_2(\mu\text{-Cl})\{\mu\text{-N(=O)-N(=O)}\}(\mu\text{-pz})]$ (**2**: $\{Ru_2(NO)_2\}^{14}$).[3a] The reversibility of this N-N bond was also observed. Treatment of **2** with protons gave an oxido-bridged complex $[(TpRu)_2(\mu\text{-Cl})(\mu\text{-O})(\mu\text{-pz})]$ (**3**), evolving N_2O. Double protonation of complex **3**, followed by exposure to NO gas, reformed complex **1**. These reactions indicate completion of the NO reduction cycle ($2NO + 2H^+ + 2e^- \rightarrow N_2O + H_2O$).[3b,c] Although NO disproportionation ($3NO \rightarrow N_2O + NO_2$) is a very common metal complex-mediated reaction,[4] the reduction reaction of NO to N_2O and H_2O has been scarcely reported,[3c,5] and is seen for metalloenzyme nitric oxide reductase (NOR).[6]

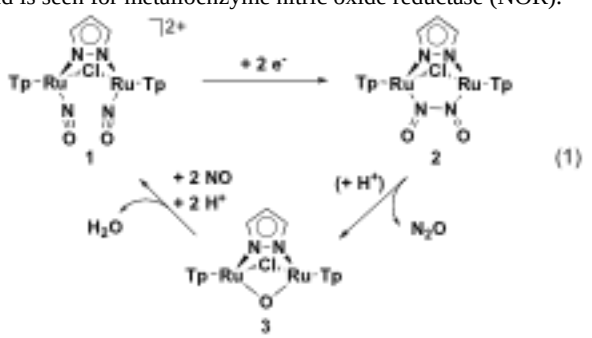

(1)

In this context, we are interested in the reactivity of a mononitrosyl ligand on dinuclear ruthenium complexes toward an additional NO molecule, including the formation of the unusual N–N coupling complex **2**. For this purpose, at first a cationic mononitrosyl dinuclear ruthenium complex $[\{TpRu(NO)\}\{TpRu(NCMe)\}(\mu\text{-Cl})(\mu\text{-pz})](BF_4)$ (**4**: $\{Ru_2(NO)\}^{12}$) was synthesized by reaction of complex **1** with NaN_3 as an NO removing reagent[7] in CH_3CN. This reaction depended on the reaction solvents. The redox reactions are also described.

Results and Discussion

The mononitrosyl complex **4** was prepared by treatment of **1** with nucleophile azide (NaN_3) in CH_3CN to remove a NO ligand, followed by coordination of the solvent molecule (Scheme 1).

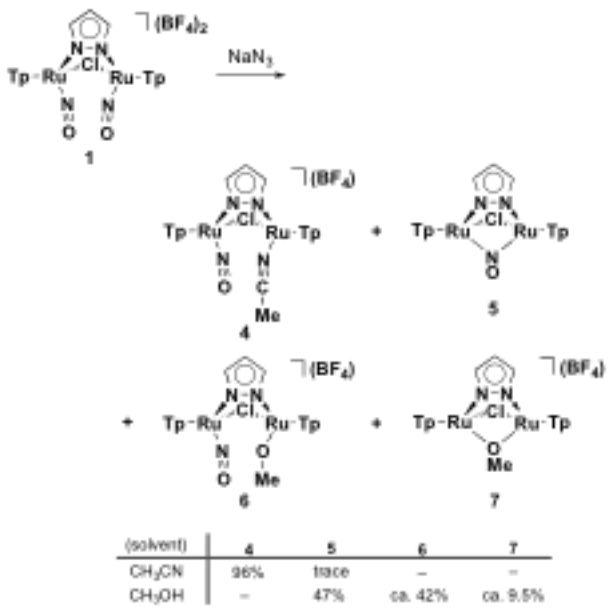

(solvent)	4	5	6	7
CH_3CN	96%	trace	–	–
CH_3OH	–	47%	ca. 42%	ca. 9.5%

Scheme 1

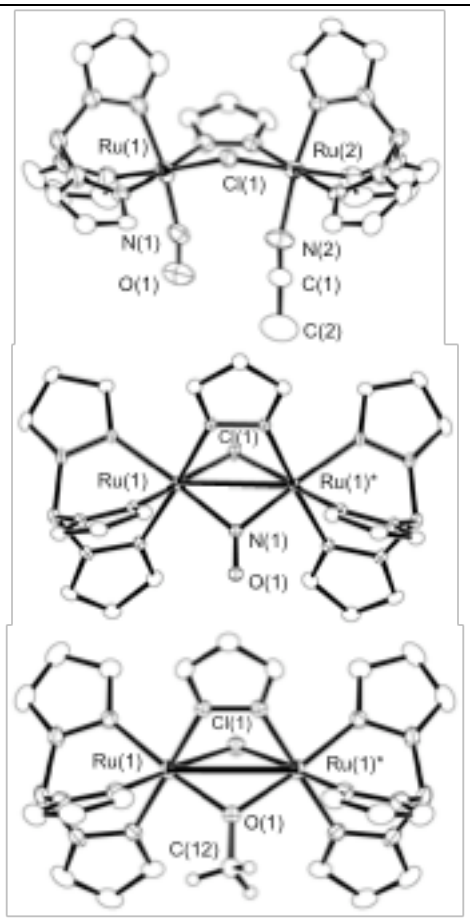

Fig. 1 Molecular structures of the cation part of **4** (top), **5** (middle), and the cation part of **7** (bottom) with thermal ellipsoids at the 50% probability level. All hydrogen atoms except for O-Me (**7**) and solvent molecules are omitted for clarity. Selected bond lengths (Å) and angles (º) for **4**: Ru(1)–N(1) = 1.813(8), Ru(2)–N(2) = 2.015(10), O(1)–N(1) = 1.145(12), N(2)–C(1) = 1.126(14), Ru(1)–N(1)–O(1) = 166.1(9), Ru(2)–N(2)–C(1) = 166.9(10). Selected bond lengths (Å) and angles (º) for **5**: Ru(1)–N(1) = 1.949(3), O(1)–N(1) = 1.209(5), Ru(1)–N(1)–Ru(1)* = 96.38(15). Selected bond lengths (Å) and angles (º) for **7**: Ru(1)–O(1) = 1.992(3), O(1)–C(12) = 1.410(7), Ru(1)–O(1)–Ru(1)* = 104.97(18).

By column chromatography, complex **4** was isolated as a dark green solid in 96% yield, concomitant with a trace amount of a nitrosyl-bridged complex $[(TpRu)_2(\mu\text{-}Cl)(\mu\text{-}NO)(\mu\text{-}pz)]$ (**5**: $\{Ru_2(NO)\}^{13}$). But the use of CH_3OH instead of CH_3CN as the reaction solvent afforded complex **5** in 47% yield. In addition, two complexes, $[\{TpRu(NO)\}\{TpRu(OMe)\}(\mu\text{-}Cl)(\mu\text{-}pz)](BF_4)$ (**6**: $\{Ru_2(NO)\}^{11}$; *ca.* 42%) and $[(TpRu)_2(\mu\text{-}Cl)(\mu\text{-}OMe)(\mu\text{-}pz)](BF_4)$ (**7**) (*ca.* 9.5%), were obtained. Complete purification of **6** and **7** was hampered by the fact that they are inseparable mutual complexes. The NO elimination reaction in CH_3OH is a complicated reaction, because the redox processes are required for the formation of **5**, **6**, and **7**. Although the ^1H NMR spectra of **5** - **7** indicate paramagnetism, the ^1H NMR spectrum of **4** shows diamagnetic signals assignable to distinct seven sets of peaks of the pyrazolyl groups (two Tp and one bridging pyrazolyl ligands), indicating an unsymmetrical dinuclear complex. The paramagnetic character of **7** indicates a weak antiferromagnetic coupling, as shown in a hydroxido-bridged dinuclear ruthenium complex $[(TpRu)_2(\mu\text{-}Cl)(\mu\text{-}OH)(\mu\text{-}pz)](BF_4)$.[3b] The IR spectra of **4** and **6** exhibit ν(NαO) bands (**4**; 1883 cm^{-1}, **6**; 1898 cm^{-1}) which

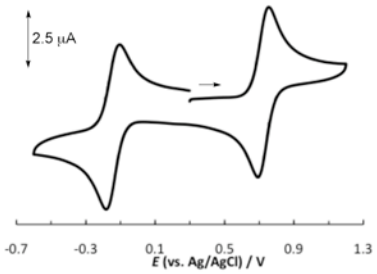

Fig. 2 Cyclic voltammogram of **4** (0.1 mM) in CH_3CN containing $^nBu_4NPF_6$ (0.1 M); working electrode: Pt; counter electrode: Pt; reference: Ag/AgCl; scan rate 50 mVs^{-1}.

Scheme 2

are lower frequencies than that of **1**,[3a] together with a ν(CαN) band (**4**; 2264 cm^{-1}). The FAB-MS spectra of **4** - **7** exhibit the parent molecular ion signals, respectively.

The structures of **4**, **5**, and **7** were confirmed by single-crystal X-ray diffraction analyses (Fig. 1). All three structures are dinuclear ruthenium complexes bridged by a chlorido and a pyrazolato ligand, but furthermore NO (for **5**) or OMe (for **7**) bridges are seen. For complex **7**, two NO ligands are removed. In complex **4**, each ruthenium is coordinated by a NO and a MeCN ligand, respectively, exhibiting the unsymmetrical structure. The N–O bond distance of **4** (1.145(12) Å; terminal) is shorter than that of **5** (1.209(5) Å; bridging), which is reasonable. The order of the Ru–Ru distances is **4** (3.7241(17) Å) > **7** (3.1596(6) Å) > **5** (2.9051(3) Å). The Ru–O distances of **7** (1.992(3) Å) are similar to those of the hydroxido-bridged complex $[(TpRu)_2(\mu\text{-}Cl)(\mu\text{-}OH)(\mu\text{-}pz)](BF_4)$ (2.0038(19) Å).[3b]

To check the redox behavior of **4**, the cyclic voltammogram was measured (Fig. 2). The CV of **4** features two reversible redox couple at -0.150 V and 0.750 V ($E_{1/2}$ *vs.* Ag/AgCl). Reductive treatment of **4** with KO_2 in CH_2Cl_2 gave the nitrosyl-bridged complex **5** in 61% yield, releasing the MeCN ligand. Moreover, oxidation of **5** with $AgBF_4$ in CH_3CN reformed **4** in 94% yield (Scheme 2), showing the reversibility. On the other hand, oxidative treatment of **4** with $AgBF_4$ in CH_2Cl_2 afforded a purple precipitate, followed by work-up to give a dicationic mononitrosyl dinuclear ruthenium complex $[\{TpRu(NO)\}\{TpRu(NCMe)\}(\mu\text{-}Cl)(\mu\text{-}pz)](BF_4)_2$ (**8**: $\{Ru_2(NO)\}^{11}$) in 65% yield. In the IR spectrum of **8**, a ν(NαO) band (1898 cm^{-1}) appears at higher frequency than that of **4**, because of the oxidation reaction. The paramagnetic complex **8** was confirmed by the X-ray structural analysis of the OH_2 ligated analog (complex **8'**), where an OH_2 ligand instead of the acetonitrile ligand coordinated to the ruthenium atom. Complex

8' was prepared by precipitation from reaction of the nitrosyl-bridged complex **5** with $AgBF_4$ in wet benzene. However, when

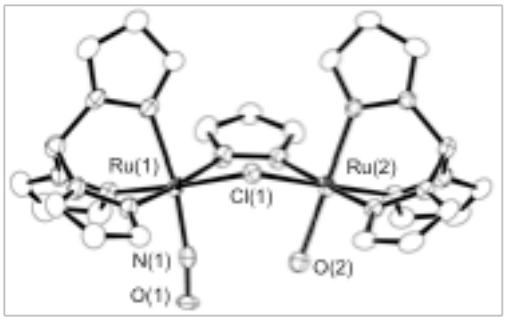

Fig. 3 Molecular structure of the cation part of **8'** with thermal ellipsoids at the 50% probability level. Minor sets of the disordered atoms and all hydrogen atoms are omitted for clarity.

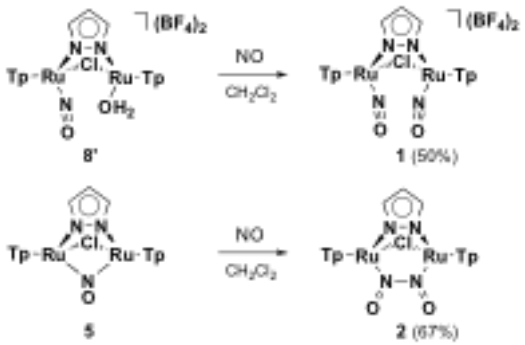

Scheme 3

this oxidation reaction was carried out in CH_3CN, only the 1 e^- oxidation product **4** was isolated. The crystallographically determined structure of **8'** is shown in Fig. 3. Unfortunately, the crystallographic disorder between NαO and OH_2 ligands causes uncertainty of the metric structural parameters, but the presence of these two ligands was established.

With the desired mononitrosyl complexes in hand, their reactions to a second NO molecule were carried out (Scheme 3). Complex **8'** ($\{Ru_2(NO)\}^{11}$) was reacted with NO (gas) for 3 h to give the dicationic dinitrosyl complex **1** ($\{Ru_2(NO)_2\}^{12}$) as a red-brown solid in 50% yield, where the OH_2 ligand of **8'** was replaced by a NO molecule. Treatment of the NO-bridged complex **5** ($\{Ru_2(NO)\}^{13}$) with NO (gas) for 3 h gave the N–N coupling complex **2** ($\{Ru_2(NO)_2\}^{14}$) as a yellow-brown solid in 67% yield, which was purified by column chromatography. Although the reaction mechanism is unclear, transformation of the bridging NO ligand to the N–N coupling form is interesting. In contrast to this, transformation of two NO molecules on dinuclear ruthenium complexes, affording *trans*-hyponitrite complexes, has been reported.[8] On the other hand, reaction of the cationic mononitrosyl ruthenium **4** ($\{Ru_2(NO)\}^{12}$) with NO (gas) did not proceed sufficiently to recover the starting complex **4** (58%), along with the formation of **1** (13%) and **2** (2.4%) which should be formed after initial redox reaction of **4** with NO radical. The reactivity of **4** indicated that the reaction scheme ($\{Ru_2(NO)\}^{12}$ (**4**) + $^{\bullet}$NO -> $\{Ru_2(NO)_2\}^{13}$) did not proceed, because the CV of **2** showed a reversible two-electron redox couple ((**2**: $\{Ru_2(NO)_2\}^{14}$) / (**1**: $\{Ru_2(NO)_2\}^{12}$)) at 0.389 V ($E_{1/2}$ *vs.* Ag/AgCl),[3a] indicating that the putative dinitrosyl complex $\{Ru_2(NO)_2\}^{13}$ is unstable. In addition, the difficulty in substituting the MeCN ligand of **4** may account for this low reactivity.

Conclusions

In conclusion, we succeeded in isolating the neutral nitrosyl-bridged complex and the cationic and dicationic mononitrosyl complexes, and showed their interconversion by chemical redox reactions. As expected from the electron count, the reactions of the nitrosyl-bridged complex **5** ($\{Ru_2(NO)\}^{13}$) and the dicationic mononitrosyl complex **8'** ($\{Ru_2(NO)\}^{11}$) with a second NO molecule resulted in the N–N coupling complex **2** ($\{Ru_2(NO)_2\}^{14}$) and the dicationic dinitrosyl complex **1** ($\{Ru_2(NO)_2\}^{12}$), respectively. On the other hand, the NO addition reaction of the cationic mononitrosyl complex **4** ($\{Ru_2(NO)\}^{12}$) did not proceed.

Experimental

General

All reactions were carried out under N_2 or Ar unless otherwise noted and subsequent work-up manipulations were performed in air. The starting material $[\{TpRu(NO)\}_2(\mu\text{-Cl})(\mu\text{-pz})](BF_4)_2$ (**1**) was prepared according to a previously reported method.[3a] Organic solvents and all other reagents were commercially available and used without further purification. NMR spectra were recorded on a Varian Gemini-300 and a JEOL JNM-AL-400 spectrometers. ^{1}H NMR chemical shifts in $CDCl_3$ or CD_3CN are quoted with respect to TMS and the deuterated solvent signal, respectively, and $^{13}C\{^1H\}$ NMR chemical shifts are quoted with respect to the deuterated solvent signal. Infrared spectra in KBr pellets were obtained on JASCO FT-IR-4100 spectrometers. Fast atom bombardment mass spectra (FAB-MS) was recorded on a JEOL JMS-700N spectrometer. Elemental analyses (C, H, N) were performed on a Perkin Elmer 2400II elemental analyzer.

Reactions of $[\{TpRu(NO)\}_2(\mu\text{-Cl})(\mu\text{-pz})](BF_4)_2$ (1) with NaN_3

NaN_3 (5.1 mg, 0.078 mmol) was added to a solution of complex **1** (50.0 mg, 0.0518 mmol) in CH_3CN (10 mL), followed by stirring for 3 h at room temperature. After evaporation to dryness, the residue was separated on column chromatography with a silica gel using a CH_2Cl_2 eluent to give $[(TpRu)_2(\mu\text{-Cl})(\mu\text{-NO})(\mu\text{-pz})]$ (**5**) as an ocher solid (trace) and a CH_2Cl_2-acetone (10/1) eluent to give $[\{TpRu(NO)\}\{TpRu(NCMe)\}(\mu\text{-Cl})(\mu\text{-pz})](BF_4)$ (**4**) as a dark green solid (44.2 mg, 96%).

When this reaction was performed in a CH_3OH reaction solvent (10 mL) using complex **1** (30.0 mg, 0.031 mmol) and NaN_3 (6.1 mg, 0.094 mmol), column chromatographic purification with a silica gel afforded complex **5** (11.1 mg, 47%; a CH_2Cl_2 eluent), $[(TpRu)_2(\mu\text{-Cl})(\mu\text{-OMe})(\mu\text{-pz})](BF_4)$ (**7**) as a green solid (2.5 mg, *ca.* 9.5%; a CH_2Cl_2-acetone (20/1) eluent), and $[\{TpRu(NO)\}\{TpRu(OMe)\}(\mu\text{-Cl})(\mu\text{-pz})](BF_4)$ (**6**) as a brown solid (11.4 mg, *ca.* 42%; a CH_2Cl_2-acetone (10/1) eluent). Complete purification of **6** and **7** was hampered by the fact that they are inseparable mutual complexes.

4: IR (KBr, pellet): ν(BH) 2520 (w); ν(C≡N) 2264 (w); ν(N≡O)

1883 (s); ν(BF) 1113–1053 (s) cm^{-1}. ^1H NMR ($CDCl_3$): δ 8.43 (d, *J* = 2.2 Hz, 1H, pz), 8.14 (d, *J* = 1.8 Hz, 1H, pz), 8.08 (d, *J* = 2.2 Hz, 1H, pz), 7.97 (d, *J* = 2.4 Hz, 1H, pz), 7.87 (d, *J* = 2.4 Hz, 1H, pz), 7.81 (d, *J* = 2.4 Hz, 1H, pz), 7.78 (d, *J* = 2.3 Hz, 1H, pz), 7.77 (d, *J* = 2.4 Hz, 1H, pz), 7.75 (d, *J* = 2.3 Hz, 1H, pz), 7.60 (d, *J* = 1.8 Hz, 1H, pz), 7.15 (d, *J* = 2.0 Hz, 1H, pz), 7.03 (d, *J* = 2.4 Hz, 1H, pz), 6.91 (d, *J* = 2.2 Hz, 1H, pz), 6.85 (d, *J* = 1.7 Hz, 1H, pz), 6.63 (t, *J* = 2.4 Hz, 1H, pz), 6.51 (t, *J* = 2.4 Hz, 1H, pz), 6.35 (t, *J* = 2.3 Hz, 1H, pz), 6.34 (t, *J* = 2.3 Hz, 1H, pz), 6.24 (t, *J* = 2.3 Hz, 1H, pz), 6.23 (t, *J* = 2.3 Hz, 1H, pz), 6.15 (t, *J* = 2.2 Hz, 1H, pz), 2.44 (s, 3H, C*H*$_3$CN). $^{13}C\{^1H\}$ NMR (CD_3CN): δ 145.6 (pz), 145.2 (pz), 145.1 (pz), 144.9 (pz), 144.8 (pz), 144.6 (pz), 143.9 (pz), 143.2 (pz), 139.7 (pz), 139.2 (pz), 138.3 (pz) 137.6 (pz), 137.4 (pz), 137.1 (pz), 110.2 (pz), 109.4 (pz), 108.6 (pz), 108.2 (pz), 108.1 (pz), 107.4 (pz), 107.3 (pz), 126.3 (CH_3CN), 5.23 (CH_3CN). FAB-MS (*m*/*z*): 802.2 ($[M]^+$), 761.2 ($[M - (CH_3CN)]^+$). Elemental analysis (%) calcd for $C_{23}H_{26}N_{16}B_3ClF_4ORu_2$: C 31.09, H 2.95, N 25.22; found: C 30.91, H 2.76, N 24.95.

5: IR (KBr, pellet): ν(BH) 2485 (w) cm^{-1}. FAB-MS (*m*/*z*): 761.1 ($[M]^+$), 694.0 ($[M - pz]^+$), 528.2 ($[Tp_2Ru]^+$). Elemental analysis (%) calcd for $C_{21}H_{23}N_{15}B_2ClORu_2$: C 33.16, H 3.05, N 27.62; found: C 33.62, H 2.86, N 27.24.

6: IR (KBr, pellet): ν(BH) 2518 (w); ν(N≡O) 1898 (s); ν(BF) 1120–1052 (s) cm^{-1}. FAB-MS (*m*/*z*): 792.0 ($[M]^+$), 762.0 ($[M - (NO)]^+$).

7: IR (KBr, pellet): ν(BH) 2514 (w); ν(BF) 1120–1050 (s) cm^{-1}. FAB-MS (*m*/*z*): 762.0 ($[M]^+$).

Redox reactions of [{TpRu(NO)}{TpRu(NCMe)}(μ-Cl)(μ-pz)](BF$_4$) (4) and [(TpRu)$_2$(μ-Cl)(μ-NO)(μ-pz)] (5)

KO_2 (7.7 mg, 0.11 mmol) was added to a solution of complex **4** (92.2 mg, 0.104 mmol) in CH_2Cl_2 (10 mL), and the mixture was stirred for 17 h at room temperature. After addition of KO_2 (7.6 mg, 0.11 mmol) and stirring for a further 7 h, column chromatographic purification with a silica gel afforded complex **5** (48.4 mg, 61%) using a CH_2Cl_2 eluent.

To a CH_2Cl_2 (10 mL) solution of complex **4** (50.0 mg, 0.0563 mmol) was added $AgBF_4$ (11.0 mg, 0.0565 mmol) in benzene (1.0 mL). After the mixture was stirred overnight and evaporated to dryness, the residue was extracted with acetone, followed by filtration. After evaporation, the residue was washed with benzene and a small amount of CH_2Cl_2 to give [{TpRu(NO)}{TpRu(NCMe)}(μ-Cl)(μ-pz)](BF$_4$)$_2$ (**8**) as a purple solid (35.9 mg, 65%).

To a CH_3CN (10 mL) solution of complex **5** (25.0 mg, 0.0329 mmol) was added $AgBF_4$ (6.4 mg, 0.033 mmol). After the mixture was stirred overnight and evaporated to dryness, the residue was separated by column chromatography with a silica gel using a CH_2Cl_2-acetone (10/1) eluent to give complex **4** (27.5 mg, 94%). On the other hand, the use of a wet benzene reaction solvent (5.0 mL), complex **5** (25.0 mg, 0.0329 mmol), and $AgBF_4$ (12.8 mg, 0.0658 mmol) resulted in a dark red purple precipitate. After stirring for 4 h and decantation of the mixture, the precipitate was washed several times with benzene to yield [{TpRu(NO)}{TpRu(OH$_2$)}(μ-Cl)(μ-pz)](BF$_4$)$_2$ (**8'**) as a red-purple solid (29.3 mg, 94%).

8: IR (KBr, pellet): ν(BH) 2523 (w); ν(N≡O) 1898 (s); ν(BF) 1121–1053 (s) cm^{-1}. FAB-MS (*m*/*z*): 802.2 ($[M]^+$), 761.1 ($[M - (CH_3CN)]^+$). Elemental analysis (%) calcd for $C_{23}H_{26}N_{16}B_4ClF_8ORu_2$: C 28.32, H 2.69, N 22.98; found: C 28.55, H 2.90, N 23.04.

8': IR (KBr, pellet): ν(BH) 2543 (w); ν(N≡O) 1915 (s); ν(BF) 1122–1053 (s) cm^{-1}. FAB-MS (*m*/*z*): 778 ($[M-1]^+$), 761.1 ($[M - (OH_2)]^+$), 694.0 ($[M - (OH_2) - pz]^+$). Elemental analysis (%) calcd for $C_{24}H_{31}N_{15}B_4Cl_7F_8O_2Ru_2$: C 23.88, H 2.59, N 17.40; found: C 24.04, H 2.27, N 17.87.

Reactivities of [{TpRu(NO)}{TpRu(NCMe)}(μ-Cl)(μ-pz)](BF$_4$) (4), [(TpRu)$_2$(μ-Cl)(μ-NO)(μ-pz)] (5), and [{TpRu(NO)}{TpRu(OH$_2$)}(μ-Cl)(μ-pz)](BF$_4$)$_2$ (8') toward NO gas

In a Schlenk flask, complex **8'** (32.0 mg, 0.0336 mmol) was dissolved in distilled CH_2Cl_2 (10 mL), followed by freeze-pump-thaw cycling for three times. After the cycling, NO gas was introduced into the Schlenk flask through a column containing KOH pellets and through an acetone/liquid N_2 (-78 ºC) cooled trap to remove impurities. The solution was exposed to NO gas for 3 h and evaporated to dryness, followed by washing with CH_2Cl_2. The resulting red-brown powder was crystallized from CH_3CN/ether to afford [{TpRu(NO)}$_2$(μ-Cl)(μ-pz)](BF$_4$)$_2$ (**1**) (16.2 mg, 50%).

Following analogous procedures to those above, reaction of complex **5** (30.7 mg, 0.0404 mmol) with NO gas in distilled CH_2Cl_2 (10 mL) afforded [(TpRu)$_2$(μ-Cl){μ-N(=O)-N(=O)}(μ-pz)] (**2**) (21.5 mg, 67%), which was purified by column chromatography.

A solution of complex **4** (41.0 mg, 0.0461 mmol) in distilled CH_2Cl_2 (10 mL) was exposed to NO gas according to the method described above. After filtration, column chromatographic purification with a silica gel gave unreacted complex **4** (23.7 mg, 58%), complex **1** (6.0 mg, 13%), and complex **2** (0.9 mg, 2.4%).

Single-crystal X-ray structural determinations

The crystallographic data are summarized in Table 1. X-ray quality single crystals were obtained from THF/ether (for **4**·$(C_4H_8O)_3$), CH_3CHCl_2/MeOH (for **5**·$(MeOH)_{1.33}$·$(CH_3CHCl_2)_{0.33}$), CH_2ClCH_2Cl/ether (for **7**·(CH_2ClCH_2Cl)), and CH_2Cl_2/hexane (for **8'**·$(CH_2Cl_2)_3$), respectively. Diffraction data were collected at -180 ºC under a stream of cold dinitrogen gas on a Rigaku RA-Micro7 HFM instrument equipped with a Rigaku Saturn724+ CCD detector by using graphite-monochromated Mo Kα radiation. The intensity images were obtained at exposure of 8 s/º (**4**·$(C_4H_8O)_3$ and **7**·(CH_2ClCH_2Cl)), 16 s/º (**5**·$(MeOH)_{1.33}$·$(CH_3CHCl_2)_{0.33}$), and 4 s/º (**8'**·$(CH_2Cl_2)_3$). The frame data were integrated using a Rigaku CrystalClear program package, and the data sets were corrected for absorption using REQAB program.

The calculations were performed with a CrystalStructure software package. The structures were solved by direct methods (for **5**·$(MeOH)_{1.33}$·$(CH_3CHCl_2)_{0.33}$, **7**·(CH_2ClCH_2Cl), and **8'**·$(CH_2Cl_2)_3$) and Patterson methods (for **4**·$(C_4H_8O)_3$), and refined on F^2 by the full-matrix least squares methods. Anisotropic refinement was applied to all non-hydrogen atoms except for three THF crystal solvents and a BF_4 group in

4·$(C_4H_8O)_3$, and the disordered minor positions (NO and O atoms) and fluorine atoms of two BF_4 groups in **8'**·$(CH_2Cl_2)_3$. For **4**·$(C_4H_8O)_3$, three fluorine atoms of a BF_4 group were disordered with an occupancy factor of 0.5/0.5. Restraints were applied to BF_4 and three THF atoms. For **5**·$(MeOH)_{1.33}$·$(CH_3CHCl_2)_{0.33}$, one MeOH, one-third MeOH, and one-third CH_3CHCl_2 crystal solvents are included. The latter two are located in the special positions, where the oxygen atom of the MeOH crystal solvent is disordered over three positions and for CH_3CHCl_2 crystal solvent the carbon and chlorine atoms are disordered over two and three positions, respectively. Three protons of the OMe group and the CH_2ClCH_2Cl crystal solvent in **7**·(CH_2ClCH_2Cl) are disordered over two positions with an occupancy factor of 50:50. For **8'**·$(CH_2Cl_2)_3$, there was a disorder between N≡O group and O (OH_2) atom with an occupancy factor of 0.7/0.3. Moreover, three fluorine atoms on each of the two BF_4 groups were disordered with an occupancy factor of 0.7/0.3. Restraints were applied to two BF_4 and three CH_2Cl_2 atoms in **8'**·$(CH_2Cl_2)_3$. Hydrogen atoms for all structures were put at calculated positions, except for B-H (**8'**·$(CH_2Cl_2)_3$), while those of the OH_2 ligand (**8'**·$(CH_2Cl_2)_3$) and the crystal solvent molecules (**4**·$(C_4H_8O)_3$, **5**·$(MeOH)_{1.33}$·$(CH_3CHCl_2)_{0.33}$, and **7**·(CH_2ClCH_2Cl)) were not included in the calculations.

Table 1 Crystallographic data for **4**·$(C_4H_8O)_3$, **5**·$(MeOH)_{1.33}$·$(CH_3CHCl_2)_{0.33}$, **7**·(CH_2ClCH_2Cl), and **8'**·$(CH_2Cl_2)_3$

	4·$(C_4H_8O)_3$	**5**·$(MeOH)_{1.33}$·$(CH_3CHCl_2)_{0.33}$	**7**·(CH_2ClCH_2Cl)	**8'**·$(CH_2Cl_2)_3$
Formula	$C_{35}H_{50}N_{16}B_3ClF_4O_4Ru_2$	$C_{23}H_{29.67}N_{15}B_2Cl_{1.67}O_{2.33}Ru_2$	$C_{24}H_{30}N_{14}B_3Cl_3F_4ORu_2$	$C_{24}H_{31}N_{15}B_4Cl_7F_8O_2Ru_2$
Fw	1104.90	836.50	947.52	1207.15
Cryst system	Triclinic	Hexagonal	Monoclinic	Monoclinic
Space group	*P*-1 (No. 2)	$P6_3/m$ (No. 176)	$P2_1/m$ (No. 11)	$P2_1/c$ (No. 14)
Color of crystal	Dark green	Dark brown	Dark brown	Dark purple
Crystal size (mm)	0.10 x 0.10 x 0.05	0.30 x 0.25 x 0.05	0.15 x 0.07 x 0.04	0.23 x 0.21 x 0.13
a (Å)	11.597(5)	19.3345(5)	9.2986(15)	11.2451(15)
b (Å)	11.793(5)	19.3345(5)	14.618(3)	11.8268(15)
c (Å)	17.685(6)	14.6049(4)	13.390(3)	33.225(5)
α (deg)	77.253(16)	90	90	90
β (deg)	75.450(17)	90	100.519(3)	98.519(3)
γ (deg)	84.730(16)	120	90	90
V (Å^3)	2281.8(16)	4728.2(3)	1789.5(5)	4369.9(10)
Z	2	6	2	4
ρ_{calc} (g cm^{-3})	1.608	1.763	1.758	1.835
μ (cm^{-1})	7.944	11.522	11.334	12.004
$2\theta_{max}$ (deg)	54.8	54.9	54.9	54.9
No. of all reflns collected	18577	30479	14890	32374
No. of unique reflns	10180	3746	4230	9940
R_{int}	0.0545	0.0197	0.0258	0.0297
No. of obsd reflns [a]	6595	3504	3692	8449
No. of parameters	494	228	257	563
R_1 [a, b]	0.0980	0.0255	0.0422	0.0571
R_w (all data)[c]	0.2782	0.0720	0.1125	0.1521
GOF (all data)[d]	1.067	1.045	1.044	1.053

[a] $I > 2\sigma(I)$. [b] $R_1 = \Sigma ||Fo| - |Fc||/\Sigma |Fo|$. [c] $Rw = \{\Sigma w (Fo^2 - Fc^2)^2/\Sigma w(Fo^2)^2\}^{1/2}$. [d] GOF = $[\{\Sigma w(Fo^2 - Fc^2)^2\}/(N_o - N_p)]^{1/2}$, where *No* and *Np* denote the number of data and parameters.

Acknowledgements

This work was supported by JSPS KAKENHI grant number 22685008 and by a Grant-in-Aid for Scientific Research from Nagasaki University.

Notes and references

Division of Chemistry and Materials Science, Graduate School of Engineering, Nagasaki University, Bunkyo-machi 1-14, Nagasaki 852-8521, Japan. Fax: +81-95-819-2684; E-mail: arikawa@nagasaki-u.ac.jp

† CCDC 939832-939835. For crystallographic data in CIF or other electronic format see DOI: 10.1039/c3dt51319j

1 (a) G. K. Lahiri and K. Wolfgang, *Dalton Trans.*, 2010, **39**, 4471–4478; (b) F. Roncaroli, M. Videla, L. D. Slep and J. A. Olabe, *Coord. Chem. Rev.*, 2007, **251**, 1903–1930; (c) S. Sarkar, B. Sarkar, N. Chanda, S. Kar, S. M. Mobin, J. Fiedler, W. Kaim and G. K. Lahiri, *Inorg. Chem.*, 2005, **44**, 6092–6099; (d) J. A. McCleverty, *Chem. Rev.*, 2004, **104**, 403–418; (e) R. G. Serres, C. A. Grapperhaus, E. Bothe, E. Bill, T. Weyhermüller, F. Neese and K. Wieghardt, *J. Am. Chem. Soc.*, 2004, **126**, 5138–5153.

2 To grasp the redox states better, the modified notation $\{M_2(NO)_x\}^n$ based on the Enemark-Feltham electron counting formalism is described, where *n* denotes the number of electrons in the two metal d and π^*_{NO} orbitals (or *n* represents the number of d electrons on the two metals when the NO is formally considered to be NO^+).

3 (a) Y. Arikawa, T. Asayama, Y. Moriguchi, S. Agari and M. Onishi, *J. Am. Chem. Soc.*, 2007, **129**, 14160–14161; (b) Y. Arikawa, N. Matsumoto, T. Asayama, K. Umakoshi and M. Onishi, *Dalton Trans.*, 2011, **40**, 2148–2150; (c) Y. Arikawa and M. Onishi, *Coord. Chem. Rev.*, 2012, **256**, 468–478.

4 (a) G. B. Richter-Addo and P. Legzdins, *Metal Nitrosyls*, Oxford University Press, New York, 1992; (b) P. C. Ford and I. M. Lorkovic, *Chem. Rev.*, 2002, **102**, 993–1017; (c) T. W. Hayton, P. Legzdins and W. B. Sharp, *Chem. Rev.*, 2002, **102**, 935–991; (d) W. B. Tolman, *Activation of Small Molecules*, Wiley-VCH, Weinheim, 2006.

5 S. Zheng, T. C. Berto, E. W. Dahl, M. B. Hoffman, A. L. Speelman and N. Lehnert, *J. Am. Chem. Soc.*, 2013, **135**, 4902–4905.

6 (a) I. M. Wasser, S. de Vries, P. Moënne-Loccoz, I. Schröder and K. D. Karlin, *Chem. Rev.*, 2002, **102**, 1201–1234; (b) B. A. Averill, *Chem. Rev.*, 1996, **96**, 2951–2964; (c) P. Girsch and S. de Vries,

Biochim. Biophys. Acta, 1997, **1318**, 202–216; (d) J. Hendriks, A. Warne, U. Gohlke, T. Haltia, C. Ludovici, M. Lübben and M. Saraste, *Biochemistry*, 1998, **37**, 13102–13109; (e) E. Pinakoulaki, S. Gemeinhardt, M. Saraste and C. Varotsis, *J. Biol. Chem.*, 2002, **277**, 23407–23413; (f) W. G. Zumft, *J. Inorg. Biochem.*, 2005, **99**, 194–215; (g) P. Tavares, A. S. Pereira, J. J. G. Moura and I. Moura, *J. Inorg. Biochem.*, 2006, **100**, 2087–2100; (h) T. Hino, Y. Matsumoto, S. Nagano, H. Sugimoto, Y. Fukumori, T. Murata, S. Iwata and Y. Shiro, *Science*, 2010, **330**, 1666–1670. (i) N. Xu, J. Yi and G. B. Richter-Addo, *Inorg. Chem.*, 2010, **49**, 6253–6266; (j) M. P. Schopfer, J. Wang and K. D. Karlin, *Inorg. Chem.*, 2010, **49**, 6267–6282.

7 F. Bottomely, *Acc. Chem. Res.*, 1978, **11**, 158–163.

8 (a) H.-C. Böttcher, M. Graf, K. Mereiter and K. Kirchner, *Organometallics*, 2004, **23**, 1269–1273; (b) T. Mayer, P. Mayer and H.-C. Böttcher, *J. Organomet. Chem.*, 2012, **700**, 41–47.